Experimental Eye Research 119 (2014) 88–96

Contents lists available at ScienceDirect

Experimental Eye Research

journal homepage: www.elsevier.com/locate/yexer

Focal damage to macaque photoreceptors produces persistent visual loss

Jennifer M. Strazzeri [a], Jennifer J. Hunter [a], Benjamin D. Masella [c], Lu Yin [a,b], William S. Fischer [a], David A. DiLoreto Jr. [a], Richard T. Libby [a,b], David R. Williams [b,c], William H. Merigan [a,b,*]

[a] Flaum Eye Institute, University of Rochester, Rochester, NY, USA
[b] Center for Visual Science, University of Rochester, Rochester, NY, USA
[c] Institute of Optics, University of Rochester, Rochester, NY, USA

ARTICLE INFO

Article history:
Received 17 August 2013
Accepted in revised form 1 November 2013
Available online 5 December 2013

Keywords:
retina
light damage
ganglion cells
macaque
adaptive optics

ABSTRACT

Insertion of light-gated channels into inner retina neurons restores neural light responses, light evoked potentials, visual optomotor responses and visually-guided maze behavior in mice blinded by retinal degeneration. This method of vision restoration bypasses damaged outer retina, providing stimulation directly to retinal ganglion cells in inner retina. The approach is similar to that of electronic visual protheses, but may offer some advantages, such as avoidance of complex surgery and direct targeting of many thousands of neurons. However, the promise of this technique for restoring human vision remains uncertain because rodent animal models, in which it has been largely developed, are not ideal for evaluating visual perception. On the other hand, psychophysical vision studies in macaque can be used to evaluate different approaches to vision restoration in humans. Furthermore, it has not been possible to test vision restoration in macaques, the optimal model for human-like vision, because there has been no macaque model of outer retina degeneration. In this study, we describe development of a macaque model of photoreceptor degeneration that can in future studies be used to test restoration of perception by visual prostheses. Our results show that perceptual deficits caused by focal light damage are restricted to locations at which photoreceptors are damaged, that optical coherence tomography (OCT) can be used to track such lesions, and that adaptive optics retinal imaging, which we recently used for in vivo recording of ganglion cell function, can be used in future studies to examine these lesions.

1. Introduction

The extreme vulnerability of photoreceptors to retinal eye disease has lead to the development of two methods for vision restoration that provide visual information directly to neurons of inner retina, bypassing degenerated photoreceptors. The first method involves optoelectronics, conveying an electrical representation of the visual stimulus to retinal ganglion cells via an array of stimulating electrodes placed above or below the ganglion cell layer, and this approach has recently been approved for therapeutic use in blind humans by the FDA (Humayun et al., 2012; Wilke et al., 2011). A second, optogenetic method, inserts light-gated channels such as channelrhodopsin into bipolar or retinal ganglion cells in order to render these cells light-sensitive and thus able to transduce visual to neural signals in place of the degenerated photoreceptors. The use of light-gated channels has proven effective in rodent animal models, restoring physiological responses to visual neurons, and pupillary and optomotor responses as well as visual guided behavior to mice previously blind due to outer retina degeneration (Bi et al., 2006; Doroudchi et al., 2011; Lagali et al., 2008). Although electronic prostheses have produced partial restoration of vision in blind humans (Wilke et al., 2011) light-gated channels may offer advantages including low cost, avoidance of potentially damaging retina surgery, and the dense spatial sampling of visual images by the many ganglion cells in primate central retina.

However, the potential efficacy of light-gated channels for restoring vision to blind humans is not understood because the rodent animal models in which this technique was developed are not ideal for studying perception. Macaques are an excellent model for evaluating human visual restoration, because, unlike

* Corresponding author. Department of Ophthalmology and Center for Visual Sciences, 575 Elmwood Avenue, University of Rochester, Rochester, NY 14642, USA. Tel.: +1 585 275 4872; fax: +1 585 473 3411.
E-mail address: billm@cvs.rochester.edu (W.H. Merigan).

0014-4835/$ – see front matter © 2014 Published by Elsevier Ltd.
http://dx.doi.org/10.1016/j.exer.2013.11.001

rodents, they share the highly specialized fovea that distinguishes primate vision from that of other species (Dacey, 1994). Also, aspects of perception critical to blinded humans such as acuity, contrast sensitivity, form and motion perception can be directly measured psychophysically in macaques (Merigan et al., 1991). In this study, we describe a primate model of focal laser treatment of retina that eliminates photoreceptors over a small region with no alteration in the number of ganglion cells overlying the eliminated photoreceptors. Because macaque vision is similar to human vision, restoration of visual perception can be measured in this model, making testing of monkey vision critical to evaluation of visual prostheses. Psychophysical measures in this study show that vision was eliminated at the location of damaged photoreceptors throughout the followup test period of approximately 7 months, but not disrupted at other nearby locations, including along fiber bundles that would indicate damage to axons of ganglion cells.

The value of macaque monkeys for evaluating vision restoration by light-gated channels is heightened by our recent finding that the function of the output neurons of the retina, retinal ganglion cells, can be monitored in living macaques by adaptive optics calcium imaging (Yin et al., 2012). This advance will permit future studies to measure both loss of RGC function following photoreceptor damage and restoration of function by visual prostheses. The present study demonstrates that structural adaptive optics retinal imaging can be carried out at the site of retinal laser lesions in the same monkey that is used for psychophysical testing.

2. Methods

Subjects. Two adult macaque monkeys were used, each weighing approximately 10 kg, of age between 4 and 5 years at the time lesions were made. Lesions were placed in the left eye (LE) of monkey 1 and the right eye (RE) of monkey 2. Head-posts and scleral eye coils were implanted in both monkeys to permit precise control of fixation locus, so that visual test stimuli could be placed relative to fixation locus with accuracy of approximately 0.1 deg, as previously described (Hayes and Merigan, 2007). This precision is necessary to test central vision because of the high sensitivity and resolution of vision near the fovea. All surgery was performed under isoflurane anesthesia, and all efforts were made to minimize discomfort. The monkeys were pair housed in an AAALAC accredited vivarium, fed ad libitum with a nutritious lab chow, supplemented with fruits and vegetables such as pomegranates and corn on the cob, and were given “browse”, leaf covered tree branches, weekly. Primate enrichment included 2 pieces of manipulata daily, puzzle feeders rotated among all animals, weekly videos and rotating access to a large, free ranging space with swings, perchs, etc. They were cared for by Laboratory Animal Medicine veterinary staff under the supervision of three full-time veterinarians, two with residence training in primatology, as well as 6 veterinary technicians, who monitor the health of the monkeys and check for signs of discomfort at least twice daily. This study was carried out in strict accordance with the recommendations in the Guide for the Care and Use of Laboratory Animals of the National Institutes of Health. The protocol was approved by the University Committee on Animal Resources of the University of Rochester (PHS assurance number: A-3292-01). At the conclusion of the experiments the monkeys were euthanized for histological examination of the retinas by administering an IV overdose of sodium pentobarbital (75 mg/kg), (death verified by thoracotomy) as recommended by the Panel on Euthanasia of the American Veterinary Medical Association.

2.1. Laser lesions

Using a Coherent Novus Omni laser, 12 laser lesions were made, 6 in each of the monkeys within less than ±7 deg of the fovea center: wavelength = 647 nm, duration = 0.02–0.2 s, and intensity = 100–260 mW (Table 1). An additional 3 lesions were made in the retina of monkey 1 to explore morphological changes associated with slightly larger lesions.

2.2. Fluorescein angiography (FA)

The time course of choroidal leakage of fluorescein was tracked for three lesions made at a single time in monkey 1 (lesions 7–9) and the six lesions made at a single time in monkey 2. FA was obtained with a Topcon TRC NW6 fundus camera on days 1, and 4 after placement of lesions in monkey 1 and on days 1, 3 and 5 in monkey 2. For each measure, 0.3 ml sodium fluorescein was injected intravenously and FA images taken for the next five minutes, and fluorescein leakage determined from images taken at approximately 5 min post-injection, when arterial and venous retinal circulation are substantial, and choroidal leakage is prominent.

2.3. Optical coherence tomography (OCT)

OCT images of retinal lesions were obtained with a Zeiss spectral domain OCT (Cirrus) approximately 24 h, 2 or 3 months, and after 6 months in the two monkeys.

2.4. Visual thresholds

The seated monkey faced a 17-inch color monitor, illustrated in Fig. 1, (Nanao, T560i), of illuminance 1.2 cd/m^2, which used only the green gun, at a distance of 57 cm. A small black fixation spot was presented at the center of the monitor, and contrast thresholds were measured for discriminating the orientation of small patches of vertical or horizontal grating displayed on the monitor. The grating targets were Gabor functions (cosinusoidal gratings multiplied by horizontal and vertical Gaussian weighting functions). The

Table 1
Description of the 15 individual laser lesions examined in this study. Lesions 1 – 6 in each monkey were made on one occasion, and then lesions 7 – 9 in monkey 1 were placed 16 months later. Power levels ranged from 100 to 260 uW, and durations of laser exposure from 10 to 200 ms, parameters that are common in clinical treatment for diabetic retinopathy or retinal edema. The diameter of the laser beam was set to 200 and 250 μm, but actual initial lesion size estimated from fundus photos ranged from approximately 250 to 420 um.

Lesion	Lesion parameters			Lesion size (μm)			
	Diameter	Power	Duration	Energy	Fundus	ONL	ONL
	(μm)	(mW)	(ms)	μW/sec	Image	OCT	Histology
Monkey 1							
1	200	260	10	2.6	254	80	57
2	200	200	20	4	329	136	78
3	200	100	100	10	358	112	60
4	200	200	20	4	336	136	95
5	200	100	50	5	291	160	129
6	200	100	50	5	306	176	90
7	250	100	200	20	390		73
8	250	100	100	10	419		279
9	250	100	200	20	375		127
Monkey 2							
1	200	200	20	4	314	136	66
2	200	100	100	10	388	181	138
3	200	100	50	5	343	115	116
4	200	200	50	4	261	146	70
5	200	100	200	20	418	284	230
6	200	260	10	2.6	0	0	0

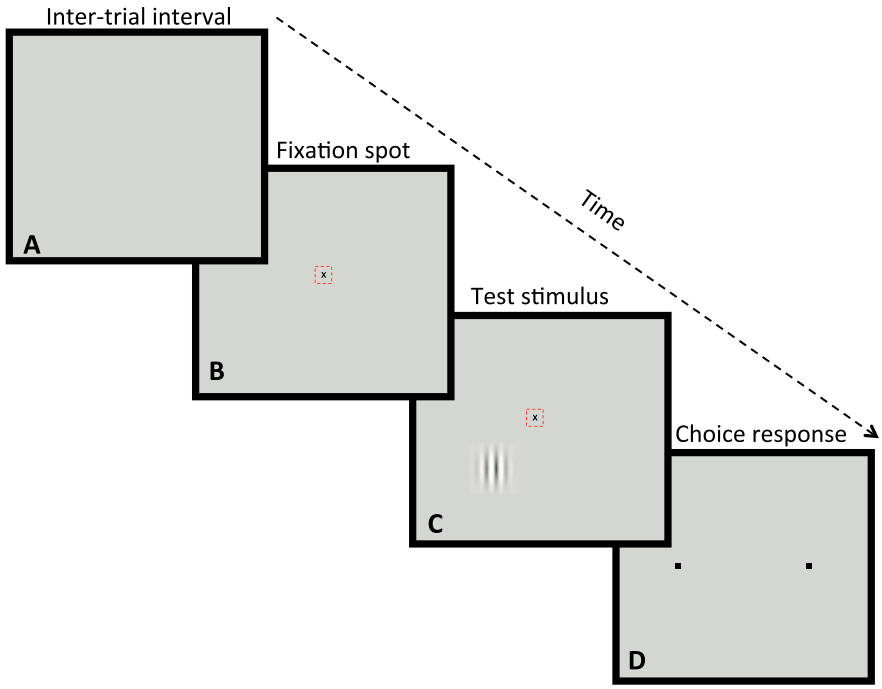

Fig. 1. *Psychophysical procedure used to test contrast thresholds.* The panels of the figure show the sequence of four conditions that were repeated in each trial. A. During the 3 s inter-trial interval the video display was blank. B. Each trial began with illumination of a small black fixation spot and the monkey was required to fixate within ±0.3 deg of the spot in order to advance to the stimulus presentation. The small dashed red box shows the location of the electronic window, not visible to the monkey, within which the monkey must fixate for 500 ms before the stimulus was presented. C. Once the fixation criterion was satisfied, a small test stimulus (vertical or horizontal Gabor stimulus) was presented for 500 ms at a location relative to the fixation spot that was chosen to test a single location in the monkey's visual field. The monkey had to maintain fixation during this period to reach the choice interval, otherwise the computer presented a 3 s tone that indicated fixation break, and the program returned to the intertrial interval (A). D. If fixation was maintained, the fixation spot and stimulus disappeared and two small black fixation response target squares appeared to the right and left of the fixation locus. The monkey was required to report that the test grating patch had been either vertical or horizontal by moving its fixation locus to one of two response squares (right box = horizontal, left box = vertical), and maintaining fixation of the response box for 10 ms. In each session of approximately 200 trials, only a single location in the visual field was tested. (For interpretation of the references to color in this figure legend, the reader is referred to the web version of this article.)

horizontal and vertical Gaussian weighting functions had equal space constants ($s = 0.15$ deg). Thus, the grating was above 37% of peak contrast (full width at the l/e point) over a region of 0.3 deg.

When the monkey fixated within 0.3″ of a black fixation spot, a test stimulus was presented at a pre-determined location in the visual field, testing only a single location in each daily session. If the monkey maintained fixation during the stimulus presentation for 0.5 s, the fixation spot and stimulus disappeared and two choice squares were presented to the right and left of fixation, so the monkey could indicate by fixating for 10 ms on one of the boxes whether the stimulus had been vertical or horizontal. Correct choices were rewarded with water, incorrect choices, fixation breaks or premature responses were followed by a 3 s beeping tone. The sequence entered a 3 s intertrial-interval following correct or incorrect choices, fixation break or premature responses.

The contrast of the stimulus was varied according to a staircase, becoming higher by one step (2 dB contrast or 0.2 octave speed) after each error, and lower with probability 0.33 after each correct choice. Daily sessions consisted of 200 trials, and thresholds were taken at 75% correct responding either by linear interpolation or by probit fits to the daily psychometric functions (Finney, 1971). All thresholds were tested monocularly in the lesioned eye (monkey 1 LE, monkey 2 RE). Visual thresholds were measured for 7 months in each monkey after placement of the initial 6 lesions.

2.5. Adaptive optics imaging

High-resolution reflection adaptive optics images of lesions were obtained in monkey 2 at the conclusion of behavioral testing in order to determine if lesion placement would compromise adaptive optics imaging, as previously described (Yin et al., 2011). Through focus images were obtained of lesions and selected images are shown to demonstrate that high signal-to-noise imaging of retinal neurons can be done following lesions.

2.6. Histology

After visual testing was complete, both monkeys were euthanized for histological examination of retinal lesions. Monkey 1 was euthanized 20 months after initial lesions were placed and Monkey 2, 30 months after lesions were placed. Retinas were initially examined as wholemounts with confocal microscopy. Following confocal microscopy of the wholemounted retina, the retina was frozen, sectioned and stained with hematoxylin and eosin, so that the general histological structure of the retina could be examined. Sections through the center of the lesion as well as neighboring sections 100 um from the lesion center were examined.

2.7. Measures of retinal scale

Lesion size and locus in the retina were determined from photographs of unfixed retinal wholemounts after euthanization. The dimensions were calculated in mm as well as degrees of visual angle (deg) from a comparison of fundus images, OCT, and psychophysical testing to the photographs of unfixed retina.

3. Results

As shown in Table 1, a total of 15 lesions were examined in this study, exploring a range of parameters that included 25% variation

in beam size, 2.6-fold variation in power and 20-fold range in duration. Lesions 1–6 were made at a single time in monkeys 1 and 2, and lesions 7–9 in monkey 1 were placed 17 weeks later. Lesions 1–6 in both monkeys were placed in a straight line, extending to about 8 degrees of eccentricity on both sides of the fovea. Initial lesion diameter, determined from fundus images, varied by less than a factor of two, with the exception of lesion 6 in monkey 2, which could not be seen in fundus images and was not visible in OCT or histology. Final lesion diameter (ONL gap size) at the time of histology varied by about 4-fold, but was relatively independent of laser parameters used to make the lesions.

Fluorescein angiography examined the integrity of retinal pigment epithelium following laser lesions. As shown in Fig. 2, fluorescein leakage was substantial at 24 h after lesion placement in all but one of the 9 lesions examined. Leakage then decreased over the next few days and was largely absent by 96 h post-lesion in monkey 1 and completely absent by 120 h in monkey 2. Leakage was minimal even at 24 h at lesion 6 in monkey 2, which involved the shortest duration laser exposure, but apart from this lesion there was no relation of laser duration and intensity to the time course of leakage. Leakage persisted slightly longer for lesions closer to the fovea in both monkeys.

OCT examined the time course of retinal changes following lesions 1–6 in the two monkeys. OCT images at 24 h after lesions (Fig. 3) showed enhanced outer nuclear layer (ONL) OCT signal that appeared to track the displacement of the near foveal Henle fibers away from the fovea. Altered OCT signal also extended toward outer retina, reaching the pigment epithelium layer (RPE). The size and location of the regions of altered OCT signal closely matched boundaries of lesions seen in fluorescein angiographs (Fig. 2) and color fundus images. No altered signal was evident in inner retina. Later OCT imaging suggested cell loss in the outer part of the ONL extending to near the RPE. At the location of each signal gap in the ONL, there was an apparent extension of the outerplexiform layer (OPL) into the ONL.

Retinal histology of the twelve 200 um diameter lesions in the two monkeys showed severe damage to outer retina but no obvious changes in the underlying inner retina. Fig. 4 shows two lesions

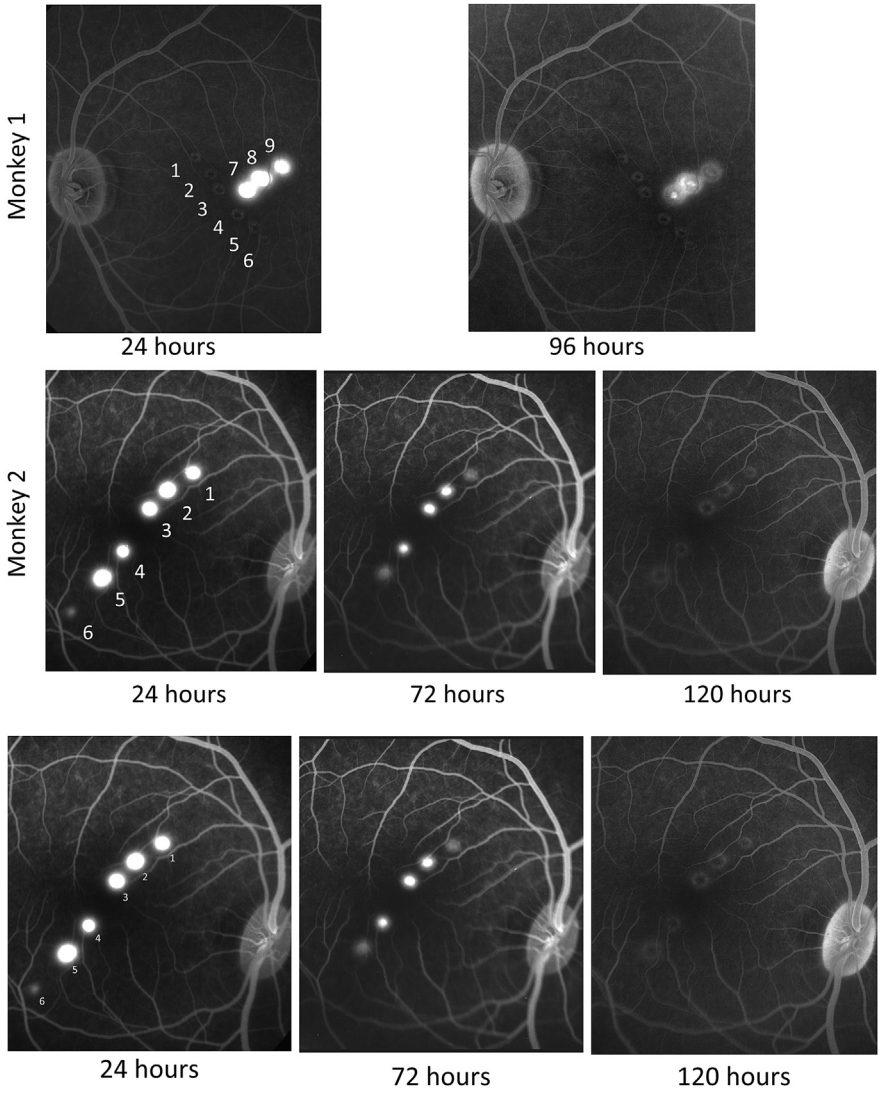

Fig. 2. *Fluorescein angiograms show leakage in the first few days after laser lesions.* Angiograms taken approximately 5 min after fluorescein injection show severe leakage of choroidal fluorescein for about 3 days. The top row shows monkey 1 and the second row monkey 2, with time after lesions extending from left to right. Each lesion is numbered as in Table 1. Monkey 1 showed severe leakage 24 h post-lesion, but leakage was markedly decreased by 96 h post-lesion. Lesions 1–6 in monkey 1 had been placed 17 weeks earlier. Monkey 2 showed severe leakage from lesions 1–5 at 24 h, but little or no leakage from lesion 6. Fluorescein leakage from lesions 1–5 was substantially decreased by 72 h and no longer present at 120 h lost-lesion.

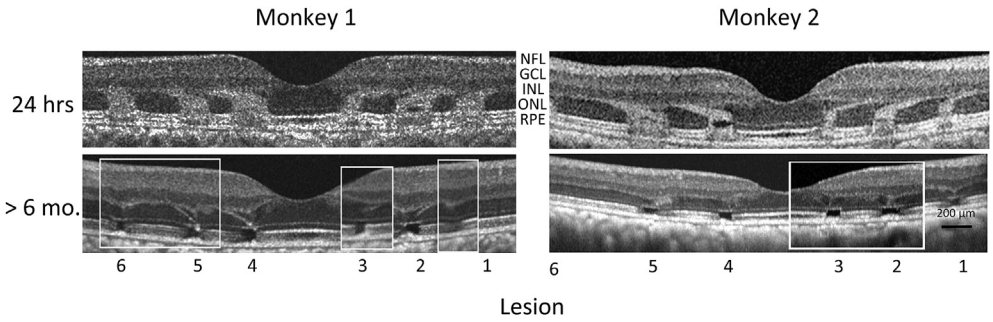

Fig. 3. *Optical coherence tomography (OCT) of lesions 1–6 in the two monkeys.* 24 h. Initial OCTs were obtained 24 h post-lesion, and show 3 lesions in each monkey on either side of the foveal pit near the center of the lesions. Altered OCT signal extends from the retinal pigment epithelium (RPE) to the outer nuclear layer, apparently tracking photoreceptor pedicles (Henle fibers), which project to bipolar cells that are displaced away from the fovea center. >6 mo. Composite OCTs are shown for each monkey, since the visibility of 6 mo. OCTs varied across individual B scans. Most lesions at this time show a gap in OCT signal from the region of photoreceptor inner and outer segments, as well as partial collapse of the outer nuclear layer (ONL), consistent with a loss of photoreceptor nuclei in the central portion of most lesions examined histologically (Figs. 4 and 5). The images >6 mo were obtained with "Selective Pixel Profiling" software (Zeiss, Jena), a method that reduces speckle noise in OCT images, and was not available when the 24 h images were obtained. This improvement in the OCT software does not affect system resolution.

from Monkey 1, illustrating the range from least observed damage (lesion 3) to the most marked damage (lesion 5) at the time of sacrifice, approximately 20 months following the lesions. Lesion 3 shows a modest gap in ONL but no gap in the inner and outer segments of photoreceptors. In contrast, lesion 5 shows a large gap in photoreceptor nuclei of the outer nuclear layer, and also in the inner and outer segments of photoreceptors. ONL was thinned on both edges of the lesion, suggesting possible migration of photoreceptor nuclei into the lesioned area. A similar gap in ONL was seen in all 6 lesions in this monkey, although the size of the gap was always approximately 50–80% smaller than the size of the initial lesion judged from fundus photos. Only three of the six lesions showed a gap in inner and outer segments of photoreceptors and none were as dramatic as that of lesion 5. Rod and cone photoreceptor somas could be distinguished in the H & E stained sections, but showed no evidence of selective damage to either rods or cones.

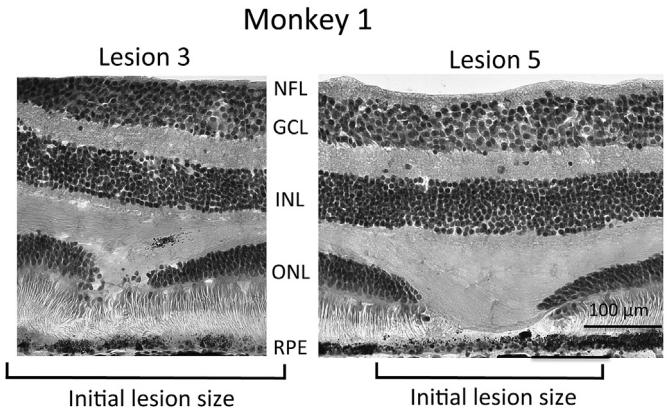

Fig. 4. *Histological appearance of two lesions in monkey 1.* Images show the range of observed gap in photoreceptor inner and outer segments; no gap in lesion 3 versus a 120 um gap in lesion 5. Of the 6 lesions examined in monkey 1, only lesion 5 showed a substantial gap in photoreceptor inner and outer segments, all other lesions showed little or no gap. The outer nuclear layer (ONL), which contains the soma of all photoreceptor cells, was interrupted by all lesions, although the gap in the ONL was smaller in all cases (see Table 1) than the initial lesion size as measured by fundus photography (Table 1). Ganglion cell layer (GCL) and inner nuclear layer (INL) showed no morphological changes at the location of lesions, nor was the nerve fiber layer (NFL) affected. We found no alteration of Muller cell morphology in neighboring vimentin stained sections. The RPE cell monolayer appeared intact across all lesions, although melanin pigment granules are reduced in some lesions (seen here in lesion 5, but not in lesion 3). Neighboring sections showed intact lipofuscin content in the monolayer of RPE cells across all lesions. Hematoxylin and eosin stain, 20×.

There was no evidence of cell loss or disorganization in either the inner nuclear layer or the ganglion cell layer. RPE cells formed a normal appearing monolayer across all lesions and inspection of neighboring unstained sections indicated that lipofuscin intensity in RPE cells was not different within lesions.

Fig. 5 shows a comparison of ex-vivo histology and in-vivo high-resolution adaptive optics imaging of lesion 5 in monkey 2. The histological appearance of the lesion (Fig. 5A) was intermediate between that of lesions 3 and 5 in monkey 1, shown in Fig. 4. Adaptive optics imaging (Fig. 5B) showed the structure of the nerve fiber layer as well as a superficial retinal vessel that crosses the lesion. Images deeper in the stack are dominated by signal from photoreceptors, which are visible surrounding the lesion, but cannot be seen in the center of the lesion. Photoreceptors at the edge of the lesion do not show the decreased density that might be expected from migration of photoreceptors toward the lesion.

Lesions 7–9 in monkey 1 involved larger laser beam diameter as well as slightly higher laser exposure parameters than the earlier 6 lesions in each money. As shown in Table 1, resulting lesion size was relatively large and the gap in the ONL was large but varied. Lesions 8 and 9 produced slight disruption of inner nuclear layer organization, not seen in any other lesions in monkey 1 or monkey 2.

The extent of perceptual improvement over months of testing differed between monkeys 1 and 2. As shown in Fig. 6, visual function in the first month after lesion placement closely matched the location and extent of funduscopically mapped lesions (red ovals). Only lesion 6 in monkey 2 showed no visual loss in the first month of testing. However, between the end of the first and end of the seventh month of testing, visual loss in monkey 2 showed almost no change, whereas loss in monkey 1 could not be detected at any locations except lesions 3 and 5. The precise time course of this recovery is not known because of the infrequent testing of individual locations, but lesion locations 1, 2, 4, and 6 in monkey 1 all showed recovery in months 2 and 3 of testing. Locations 3 and 5 in monkey 1 were tested repeatedly throughout the 1–7 month testing period and showed stable loss. No evidence was found of visual loss beyond the region of outer retina affected by the laser exposure, indicating no substantial effects involving lateral interaction in the retina or nerve fiber defects.

An important question for this study is whether visual loss was due only to the histologically observed damage to outer retina, or if inner retina may also have been compromised. Potential damage to inner retina could result from one of two mechanisms; direct damage to cells or axons caused by the passage of the laser through inner retina, or later damage caused by degeneration of inner retina

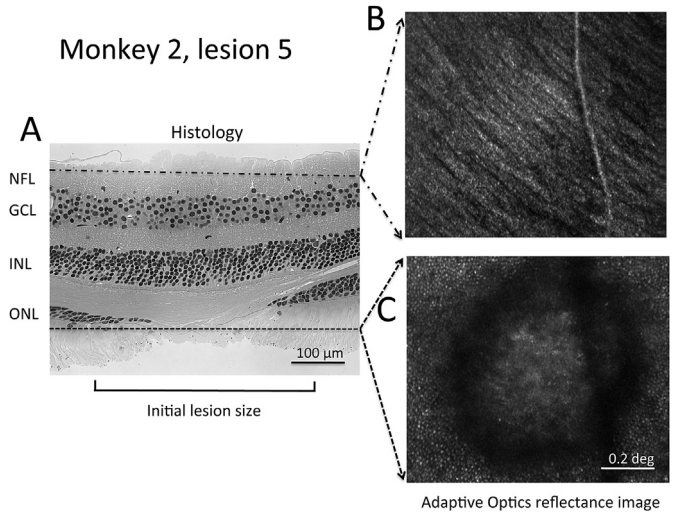

Fig. 5. *Histology and AO images of lesion 5 in monkey 2.* Comparison of a histological section through lesion 5 in monkey 2 to two images from a through-focus stack of in-vivo AO images of the same region obtained approximately 2 months before euthanasia. A. Section through lesion 5 that illustrates no apparent change in inner retinal layers (upper part of the image) but interruption of the outer nuclear layer (ONL), and the presence of photoreceptor inner and outer segments extending farther into the lesion that the ONL. B. In vivo adaptive optics image showing superficial nerve fiber layer, and C. photoreceptors surrounding the lesion. Hematoxylin and eosin stain, 20×.

subsequent to loss of outer retina input. Placement of lesions near the fovea helped clarify the first mechanism, because the marked displacement of near foveal retinal ganglion cells away from the photoreceptors that provide their input would produce two foci of visual loss if both inner and outer retina were damaged by the laser. Fig. 7 illustrates RGC displacement from outer retina lesion location for monkey 2 with black curved arrows. Predicted visual loss should correspond to the location of pink ovals (funduscopically observed lesion locations) if the loss were due only to outer retina damage. As Fig. 7 shows, the visual loss (blue dots) associated with lesions 1–5 in monkey 2 (lesion 6 produced no visual loss) was discreet and closely matched the loss expected from outer retina damage only. Dashed circles show the locus of loss expected if inner retina had been damaged by the laser exposure, locations inconsistent with the observed loss. The data of monkey 1 was less ideal for this analysis because there were only two persistent loci of visual loss, but is nonetheless consistent with this finding.

4. Discussion

This study demonstrated that primate inner retina is relatively spared by severe focal light exposure that causes degeneration of photoreceptors and permanent loss of vision. In this study, we tested a four-fold range of laser energy in order to identify parameters for inducing permanent focal lesions in macaque, and the degree of permanent visual loss was relatively independent of treatment parameters. Despite the degeneration of outer retina and persistent vision loss observed here, visual function was preserved at laser-treated locations where ganglion cells are displaced from the photoreceptors that provide their input. These results suggest that focal laser lesions in the macaque could provide a primate animal model for exploring restoration of visual function in human eye disease by direct activation of inner retinal neurons to treat the large number of eye diseases that produce initial damage to outer retina. This approach could be used to test either optoelectronic

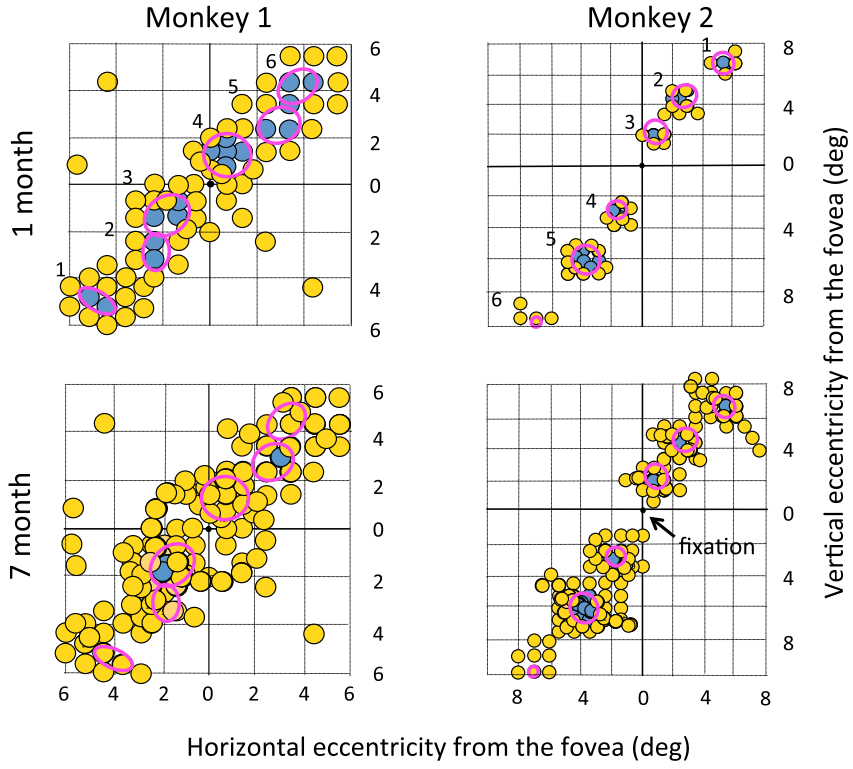

Fig. 6. *Visual performance of the two monkeys at 1 month and 7 months after lesions.* Visual orientation discrimination performance across the visual field surrounding lesions 1–6 in monkeys 1 and 2, in the first month following lesions and cumulatively to the 7th month following lesions. Red ovals show the location and size of lesions determined by fundus photography immediately after lesions, and numbers to the left of the ovals show the lesion number (Table 1). Data points show the result of contrast sensitivity testing, yellow points represent performance above 75% correct, indicating locations with visual function, and blue points represent performance below 75% correct, indicating impaired or absent vision. Each data point is approximately 0.8 deg in diameter, a conservatively large representation of the effective size of the Gabor patch of grating that was ±0.3 deg in standard deviation.

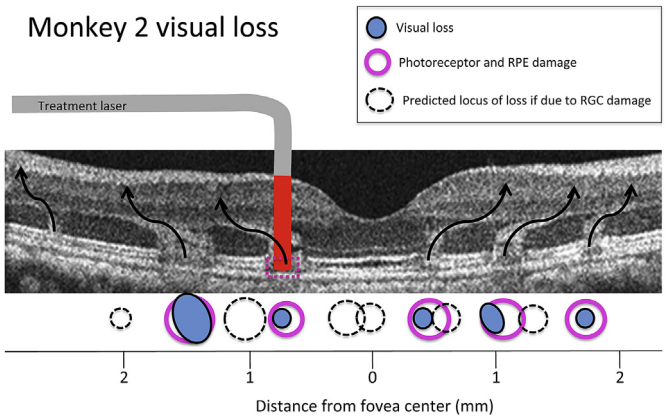

Fig. 7. *Retinal location of visual loss in monkey 2.* Mapping of the actual locations of visual loss in monkey 2, (blue circles) and the locus of lesions 1–6 determined from fundus images, OCT imaging and histology, illustrated on the OCT of this monkey taken 24 h after lesion placement. Curved arrows show the approximate flow of visual information from photoreceptors to retinal ganglion cells, based on previous anatomical studies (Schein, 1988) and matched to the altered OCT signal in the ONL that was visible 24 h post-lesion. The cartoon of laser exposure shows that red laser illumination penetrated vertically through the retina. Light-induced damage to the photoreceptors and RPE cells of the outer retina (pink circles) match the locus of visual loss measured psychophysically in lesions 1–6 (blue circles), suggesting that outer retina damage underlies visual loss. If visual loss instead resulted from damage to ganglion cells, through which the laser passed, in the inner retina, the predicted locus of loss would correspond to the dashed circles.

prostheses (Humayun et al., 2012; Wilke et al., 2011) or optogenetic approaches (Bi et al., 2006; Doroudchi et al., 2011; Lagali et al., 2008) to restoring vision after damage to outer retina.

4.1. Mechanisms of photic injury involved in this study

The degeneration of outer retina with relative sparing of inner retina observed here is consistent with previous observations that outer retina is preferentially damaged by long wavelength light, whereas shorter wavelength light damages all retinal layers from nerve fiber layer to RPE (Smiddy et al., 1984). Similar observations were reported in rabbit retina (Sher et al., 2010) with the use of short pulsed green laser. The mechanism of damage in this study is likely thermal, involving heating of the light absorbing layers of the retina, RPE and photoreceptors (Roider et al., 1993). However, we cannot rule out additional photochemical damage (van Norren and Gorgels, 2011) in which damage is independent of increased retinal temperature.

4.2. Retinal pigment epithelium

Photoreceptors and RPE cells are most vulnerable to light damage because of the high level of photic absorption by these cells. However, RPE cells in mammalian retina may recover from photic injury since they undergo proliferation in response to a variety of insults, including surgical removal (Valentino et al., 1995), retinal detachment (Fisher et al., 1991) and laser-light exposure (Smiddy et al., 1986). RPE regeneration requires only a few days to repopulate even large areas of RPE loss with a monolayer of RPE cells (Bulow, 1978; Valentino et al., 1995), and the time course of RPE regeneration parallels the cessation of leakage of choroidal fluorescein into the retina (Lopez et al., 1995). Thus, the rapid elimination of choroidal leakage observed in this study could reflect repopulation of the laser-damaged areas by new RPE cells. However we have no direct evidence that the RPE cells that completely tiled retinal lesions at the time of histology in this study did not either recover from laser damage or migrate into the lesioned area from the surrounding retina. Histological evidence in both monkeys showed that RPE cells covering all laser lesions appeared grossly normal in their monolayer pattern, cell size and lipofuscin content. These features suggest that at the time of histology RPE cells were healthy at these locations, but we did not evaluate their function, which in normal retina includes an important role in photopigment regeneration (especially in rod photoreceptors), and phagocytosis of outer segment discs (Strauss, 2005). Previous studies of RPE cells in young and old human retina showed moderate numbers of apoptotic RPE cells, but unchanged density of foveal RPE cells, suggesting possible migration or regeneration of RPE cells in central retina (Del Priore et al., 2002).

4.3. Photoreceptors

Studies in a variety of animal models have shown that photoreceptors (PR) are very sensitive to light-induced degeneration, but they do not undergo proliferation (Fisher et al., 1991). In laser-treated rabbit retina, PRs migrate into lesion sites, markedly reducing lesion size, and in some cases completely eliminating the gap in PRs (Paulus et al., 2008; Sher et al., 2013, 2010). Furthermore, multielectrode recordings of ganglion cells above lesion sites show progressive recovery of ganglion cell physiological responses (Leung et al., 2010; Sher et al., 2013, 2010). Limited migration of PRs into laser lesions has also been reported in the rat (Busch et al., 1999), with PR inner and outer segments completely covering retinal lesions of 200 μm diameter, but not larger lesions of 400 or 800 μm diameter. In the present study, despite partial filling in of lesions by inner and outer segments of PRs, gaps persisted in PR somas in the ONL in all lesions. Busch et al. found thinning of the rat ONL at the borders of lesions, a pattern also seen in the present study, and concluded that it represented partial migration of ONL into lesions. Migration of photoreceptors, with thinning of the ONL, has also been reported in young dogs in a model of retinitis pigmentosa that initially produces scattered patches of PR loss and ONL gaps (Beltran et al., 2009). Over time the PR loss disappeared and ONL thinned, while gaps in the ONL disappeared. These earlier results suggest that PR migration and visual recovery can follow outer retina lesions, at least in younger animals, raising the possibility of adult plasticity in the recovered response of overlying RGCs, as was recently reported in rabbit by Sher et al. (2010).

4.4. Inner retina

Relative preservation of inner retinal neurons in this study was suggested by the observation of no visible neuronal loss in either the ganglion cell layer or the inner nuclear at or near the lesions. However, future studies of ganglion cell recovery due to insertion of light-gated channels will require thorough evaluation of the physiology of these neurons, and this can be done with in vivo adaptive optics imaging (see below). It is expected that replacement of neural input by channelrhodopsin will substantially alter neuronal physiology, and such changes will need to be distinguished from possible “remodeling” of RGCs and bipolar cells in inner retina, a degenerative change which has earlier been found to follow degeneration of outer retina in both rodent models of eye disease and human retinal degeneration (Jones et al., 2003; Marc et al., 2007). In this future study we will avoid light damage from the visual stimulus used to activate channelrhodopsin by measuring intensity response functions for individual RGCs driven by channelrhodopsin (Yin et al., 2012) and using the minimal effective light. We expect that RGCs can be activated by channelrhodopsin with 1×10^{15} photons/sec/cm^2 (408 μJ/cm^2) (Bi et al., 2006) approximately 5000 fold below the ANSI maximum

permissible exposure (MPE) for 488 nm light (American National Standards Institute, 2007). The recent study by Sher and co-workers (Sher et al., 2013) examined likely restoration of function to RGCs by in vitro recording of RGC function comparing 2 days to 2 months after placement of laser lesions. In their study, 2 month recovery produced complete closing up of the outer retina at the site of 200 um diameter lesions, resulting in normal function of all RGCs overlying the lesions. Such closing up of the ONL was not observed in the approximately 200 um diameter lesions in the present study despite the 20 and 30 month recovery time of the two monkeys studied. The failure of outer retina lesions to close up in the present study could reflect the species difference (macaque versus rabbit) or possibly the proximity of lesions in the present study to the fovea, which is dominated by midget RGCs whose receptive field center receives input from only a single cone (McMahon et al., 2000). The Sher study also did not find evidence of inner retina remodeling above the site of retinal lesions, a finding that could reflect either the brief duration of the loss of photoreceptor input or the small size of the lesions, since inner retina remodeling is blocked by islands of surviving photoreceptors (Jones et al., 2003). Possible preservation of inner retina in the present study is unlikely due to short survival time since the monkeys survived at least 20 months. However, it may reflect persistent input of photoreceptors around the lesion to inner retina, since the diameter of lesions in this study is small compared to the size of dendritic fields of the larger cells in macaque inner central retina (Rodieck and Watanabe, 1993).

4.5. Visual loss and partial recovery in the macaque

The orientation discrimination visual thresholds measured here used a very small stimulus to examine visual perception locally, with the 0.3 deg diameter of the high-contrast portion of the stimulus. This stimulus tests pattern perception, not the less informative flash detection which could be mediated by scattered light from stimuli presented within a scotoma to surrounding regions of normal retina. This is a conservative indicator of visual performance, and shows that the 7-month performance of the two monkeys (Fig. 5) was excellent, except at tiny locations in the visual field. Because the size of visual scotomata produced by all lesions was very small, these lesions would be difficult to detect with microperimetry if they were present in a human retina, thus they are unlikely to be apparent to the subject. Failure to measure residual visual loss at 4 of the 6 lesion locations in monkey 1 could reflect inability to detect vision defects smaller than the stimulus size, since all lesions in monkey 1 showed a gap in the ONL at the time of histology.

4.6. Recovery of human visual function after light damage

The present results show that recovery of visual function in laser-exposed macaques may require weeks. Visual loss from excess light exposure in humans (Calkins and Hochheimer, 1980) can recover rapidly or slowly in different cases, suggesting the involvement of different mechanisms of damage. Visual loss from slit lamp examination (Ghafour et al., 1984) or indirect ophthalmoscopy (Fariza and Castellote, 1993) recovers in a few hours to several days, suggesting mediation by retinal light adaptation or very rapid recovery of retinal cells. On the other hand, the visual loss and retinal scarring observed in 18 patients that viewed a solar eclipse required weeks to months to heal, and often produced permanent damage (MacFaul, 1969). Retinal light damage produced by the illumination used during eye surgeries such as cataract removal (Knox Cartwright et al., 2007; Lessel et al., 1991) can produce long lasting defects in focal electroretinogram or visual perimetry, although loss following threshold laser photocoagulation in human subjects (Roider et al., 1999) often resolved from one week to a few months after treatment. The success of high-resolution OCT in examining retinal cellular structure in this study suggests that this method may be effective for detecting outer retinal damage in humans.

4.7. In future studies in vivo adaptive optics imaging may track RPE and photoreceptor plasticity as well as restoration of RGC function by light-gated channels

The present study suggested that lesion size may decrease over time in primate retina as has been previously reported for rat (Busch et al., 1999) and rabbit (Sher et al., 2013). In future studies, it will be important to track the time course of plasticity in response to the lesion itself and to differentiate such changes from those produced by visual prostheses. The use of in vivo adaptive optics imaging will permit these studies. The location of individual cone and rod photoreceptors can be imaged (Dubra et al., 2011; Liang and Williams, 1997) in order to track any migration into lesion locations. Individual RPE cells can also be imaged, both within and at the border of lesions using the distinctive pattern of lipofuscin autofluorescence that makes them visible (Morgan et al., 2009). Finally, recovery of function of retinal ganglion cells (Sher et al., 2013) can be tracked over the weeks following the lesion using the FACILE (functional adaptive optics cellular imaging in the living eye) method we have previously described (Yin et al., 2013) (Yin et al., 2012). This experiment can show both the nature and time course of photoreceptor and ganglion cell plasticity in response to focal retinal lesions as well as the effect of intervention with visual prostheses.

Author contributions

J. M. S. and W.H.M. designed the research, J. J. H., B. D. M. and L.Y. performed the AO imaging experiments and analyzed the data, W. S. F. performed OCT imaging, D. A. D. made laser lesions, J. M. S. carried out behavioral experiments, R. T. L. supervised histology, J. M. S. and W.H.M. wrote the paper and all authors were involved in modifying it.

Grant support

This work was supported by NIH research grants – EY019375, NDC 5PN2EY018241; EY021166, EY004367, BRP-EY014375, and NIH Core Grant –EY001319.

Acknowledgments

We thank Thurma McDaniel and Tracey Bubel (Center for Visual Science, University of Rochester) for assistance with histology.

References

American National Standards Institute, 2007. American National Standard for safe use of lasers. In: Anonymous American National Standard for Safe Use of Lasers. American National Standards Institute; Laser Institute of America, Orlando, FL.
Beltran, W.A., Acland, G.M., Aguirre, G.D., 2009. Age-dependent disease expression determines remodeling of the retinal mosaic in carriers of RPGR exon ORF15 mutations. Investig. Ophthalmol. Vis. Sci. 50, 3985–3995.
Bi, A., Cui, J., Ma, Y.P., Olshevskaya, E., Pu, M., Dizhoor, A.M., Pan, Z.H., 2006. Ectopic expression of a microbial-type rhodopsin restores visual responses in mice with photoreceptor degeneration. Neuron 50, 23–33.
Bulow, N., 1978. The process of wound healing of the avascular outer layers of the retina. Light- and electron microscopic studies on laser lesions of monkey eyes. Acta Ophthalmol., 7–60. Supplementum.
Busch, E.M., Gorgels, T.G., Van Norren, D., 1999. Filling-in after focal loss of photoreceptors in rat retina. Exp. Eye Res. 68, 485–492.

Calkins, J.L., Hochheimer, B.F., 1980. Retinal light exposure from ophthalmoscopes, slit lamps, and overhead surgical lamps. An analysis of potential hazards. Investig. Ophthalmol. Vis. Sci. 19, 1009–1015.
Dacey, D.M., 1994. Physiology, morphology and spatial densities of identified ganglion cell types in primate retina. Ciba Found. Symp. 184, 12–28. Discussion 28–34, 63–70.
Del Priore, L.V., Kuo, Y.H., Tezel, T.H., 2002. Age-related changes in human RPE cell density and apoptosis proportion in situ. Investig. Ophthalmol. Vis. Sci. 43, 3312–3318.
Doroudchi, M.M., Greenberg, K.P., Liu, J., Silka, K.A., Boyden, E.S., Lockridge, J.A., Arman, A.C., Janani, R., Boye, S.E., Boye, S.L., Gordon, G.M., Matteo, B.C., Sampath, A.P., Hauswirth, W.W., Horsager, A., 2011. Virally delivered channelrhodopsin-2 safely and effectively restores visual function in multiple mouse models of blindness. Mol. Ther. J. Am. Soc. Gene Ther. 19, 1220–1229.
Dubra, A., Sulai, Y., Norris, J.L., Cooper, R.F., Dubis, A.M., Williams, D.R., Carroll, J., 2011. Noninvasive imaging of the human rod photoreceptor mosaic using a confocal adaptive optics scanning ophthalmoscope. Biomed. Opt. Expr. 2, 1864–1876.
Fariza, E., Castellote, M., 1993. Clinical light damage by indirect ophthalmoscopy. N. Engl. J. Med. 329, 1505–1507.
Finney, D.J., 1971, third ed.. Probit Analysis University Press, Cambridge Eng.
Fisher, S.K., Erickson, P.A., Lewis, G.P., Anderson, D.H., 1991. Intra retinal proliferation induced by retinal detachment. Investig. Ophthalmol. Vis. Sci. 32, 1739–1748.
Ghafour, I.M., Foulds, W.S., Allan, D., 1984. Short-term effect of slit-lamp illumination and argon laser light on visual function of diabetic and non-diabetic subjects. Br. J. Ophthalmol. 68, 298–302.
Hayes, R.D., Merigan, W.H., 2007. Mechanisms of sensitivity loss due to visual cortex lesions in humans and macaques. Cereb. Cortex 17, 1117–1128.
Humayun, M.S., Dorn, J.D., da Cruz, L., Dagnelie, G., Sahel, J.A., Stanga, P.E., Cideciyan, A.V., Duncan, J.L., Eliott, D., Filley, E., Ho, A.C., Santos, A., Safran, A.B., Arditi, A., Del Priore, L.V., Greenberg, R.J., 2012. Interim results from the international trial of second sight's visual prosthesis. Ophthalmology 119, 779–788.
Jones, B.W., Watt, C.B., Frederick, J.M., Baehr, W., Chen, C.K., Levine, E.M., Milam, A.H., Lavail, M.M., Marc, R.E., 2003. Retinal remodeling triggered by photoreceptor degenerations. J. Comp. Neurol. 464, 1–16.
Knox Cartwright, N.E., Tole, D.M., Haynes, R.J., Males, J.J., Dick, A.D., Mayer, E.J., 2007. Recovery from macular phototoxicity after corneal triple procedure. Cornea 26, 102–104.
Lagali, P.S., Balya, D., Awatramani, G.B., Munch, T.A., Kim, D.S., Busskamp, V., Cepko, C.L., Roska, B., 2008. Light-activated channels targeted to ON bipolar cells restore visual function in retinal degeneration. Nat. Neurosci. 11, 667–675.
Lessel, M., Thaler, A., Heilig, P., Jantsch, W., Scheiber, V., 1991. Intra operative retinal light damage reflected in electrophysiologic data. Doc. Ophthalmol. Adv. Ophthalmol. 76, 323–333.
Leung, L.-S.B., Leng, T., Paulus, Y.M., Nomoto, H., Gariano, R.F., Sher, A., Palanker, D., 2010. Restorative retinal photocoagulation. Investig. Ophthalmol. Vis. Sci. 51, 5579.
Liang, J., Williams, D.R., 1997. Aberrations and retinal image quality of the normal human eye. J. Opt. Soc. Am. A Opt. Imag. Sci. Vis. 14, 2873–2883.
Lopez, P.F., Yan, Q., Kohen, L., Rao, N.A., Spee, C., Black, J., Oganesian, A., 1995. Retinal pigment epithelial wound healing in vivo. Arch. Ophthalmol. 113, 1437–1446.
MacFaul, P.A., 1969. Visual prognosis after solar retinopathy. Br. J. Ophthalmol. 53, 534–541.
Marc, R.E., Jones, B.W., Anderson, J.R., Kinard, K., Marshak, D.W., Wilson, J.H., Wensel, T., Lucas, R.J., 2007. Neural reprogramming in retinal degeneration. Investig. Ophthalmol. Vis. Sci. 48, 3364–3371.
McMahon, M.J., Lankheet, M.J., Lennie, P., Williams, D.R., 2000. Fine structure of parvocellular receptive fields in the primate fovea revealed by laser interferometry. J. Neurosci. Off. J. Soc. Neurosci. 20, 2043–2053.
Merigan, W.H., Katz, L.M., Maunsell, J.H., 1991. The effects of parvocellular lateral geniculate lesions on the acuity and contrast sensitivity of macaque monkeys. J. Neurosci. Off. J. Soc. Neurosci. 11, 994–1001.
Morgan, J.I.W., Dubra, A., Wolfe, R., Merigan, W.H., Williams, D.R., 2009. In Vivo autofluorescence imaging of the human and macaque retinal pigment epithelial cell mosaic. Investig. Ophthalmol. Vis. Sci. 50, 1350–1359.
Paulus, Y.M., Jain, A., Gariano, R.F., Stanzel, B.V., Marmor, M., Blumenkranz, M.S., Palanker, D., 2008. Healing of retinal photocoagulation lesions. Investig. Ophthalmol. Vis. Sci. 49, 5540–5545.
Rodieck, R.W., Watanabe, M., 1993. Survey of the morphology of macaque retinal ganglion cells that project to the pretectum, superior colliculus, and parvicellular laminae of the lateral geniculate nucleus. J. Comp. Neurol. 338, 289–303.
Roider, J., Brinkmann, R., Wirbelauer, C., Laqua, H., Birngruber, R., 1999. Retinal sparing by selective retinal pigment epithelial photocoagulation. Arch. Ophthalmol. 117, 1028–1034.
Roider, J., Hillenkamp, F., Flotte, T., Birngruber, R., 1993. Microphotocoagulation: selective effects of repetitive short laser pulses. Proc. Natl. Acad. Sci. U. S. A. 90, 8643–8647.
Schein, S.J., 1988. Anatomy of macaque fovea and spatial densities of neurons in foveal representation. J. Comp. Neurol. 269, 479–505.
Sher, A., Jones, B.W., Huie, P., Paulus, Y.M., Lavinsky, D., Leung, L.S., Nomoto, H., Beier, C., Marc, R.E., Palanker, D., 2013. Restoration of retinal structure and function after selective photocoagulation. J. Neurosci. Off. J. Soc. Neurosci. 33, 6800–6808.
Sher, A., Leung, L.-S., Leng, T., Nomoto, H., Paulus, Y., Gariano, R., Jones, B.W., Litke, A.M., Palanker, D.V., 2010. Retinal plasticity and restoration of function after photocoagulation. Investig. Ophthalmol. Vis. Sci. 51, 2482.
Smiddy, W.E., Fine, S.L., Quigley, H.A., Dunkelberger, G., Hohman, R.M., Addicks, E.M., 1986. Cell proliferation after laser photocoagulation in primate retina. An autoradiographic study. Arch. Ophthalmol. 104, 1065–1069.
Smiddy, W.E., Fine, S.L., Quigley, H.A., Hohman, R.M., Addicks, E.A., 1984. Comparison of krypton and argon laser photocoagulation. Results of stimulated clinical treatment of primate retina. Arch. Ophthalmol. 102, 1086–1092.
Strauss, O., 2005. The retinal pigment epithelium in visual function. Physiol. Rev. 85, 845–881.
Valentino, T.L., Kaplan, H.J., Del Priore, L.V., Fang, S.R., Berger, A., Silverman, M.S., 1995. Retinal pigment epithelial repopulation in monkeys after submacular surgery. Arch. Ophthalmol. 113, 932–938.
van Norren, D., Gorgels, T.G., 2011. The action spectrum of photochemical damage to the retina: a review of monochromatic threshold data. Photochem. Photobiol. 87, 747–753.
Wilke, R., Gabel, V.P., Sachs, H., Bartz Schmidt, K.U., Gekeler, F., Besch, D., Szurman, P., Stett, A., Wilhelm, B., Peters, T., Harscher, A., Greppmaier, U., Kibbel, S., Benav, H., Bruckmann, A., Stingl, K., Kusnyerik, A., Zrenner, E., 2011. Spatial resolution and perception of patterns mediated by a subretinal 16-electrode array in patients blinded by hereditary retinal dystrophies. Investig. Ophthalmol. Vis. Sci. 52, 5995–6003.
Yin, L., Geng, Y., Osakada, F., Sharma, R., Cetin, A.H., Callaway, E.M., Williams, D.R., Merigan, W.H., 2013. Imaging light responses of retinal ganglion cells in the living mouse eye. J. Neurophysiol. 109, 2415–2421.
Yin, L., Greenberg, K., Hunter, J.J., Dalkara, D., Kolstad, K.D., Masella, B.D., Wolfe, R., Visel, M., Stone, D., Libby, R.T., Diloreto Jr., D., Schaffer, D., Flannery, J., Williams, D.R., Merigan, W.H., 2011. Intravitreal injection of AAV2 transduces macaque inner retina. Investig. Ophthalmol. Vis. Sci. 52, 2775–2783.
Yin, L., Masella, B., Dalkara, D., Flannery, J.G., Schaffer, D.G., Williams, D.R., Merigan, W.H., 2012. In vivo imaging of ganglion cell physiology in macaque fovea using a calcium indicator. Optical Society of America Fall Vision Meeting J. Vis. 12 (14). Rochester NY.